Chalcogenide Letters Vol. 21, No. 1, January 2024, p. 39 - 51

Theoretical study on the elastic and thermodynamic properties of CdS

G. Hao[a,*], H. J. Hou[a], S. R. Zhang[b], L. H. Xie[c]
[a]*School of Materials Science and Engineering, Yancheng Institute of Technology, Yancheng, 224051, China*
[b]*School of Physics, Electronics and Intelligent Manufacturing, Huaihua University, Huaihua, 418008, China*
[c]*School of Physics and Electronic Engineering, Sichuan Normal University, Chengdu, 610066, China*

The physical properties of CdS is calculated by using the first principles pseudopotential plane wave method based on density functional theory (DFT). The calculated lattice parameters and elastic constants agree well with other theoretical values, and the crystal is determined to be structurally stable by the Born mechanical stability condition. The Debye temperature, Grüneisen parameters, heat capacity and thermal expansion coefficient of CdS under high temperature and high pressure were studied successfully by using the quasi-harmonic Debye model. The influence of pressure on thermal expansion coefficient and Debye temperature is greater than that of temperature. The heat capacity decreases with the increase of pressure. At high temperature and high pressure, the heat capacity approaches the Dulong-Petit limit.

(Received October 27, 2023; Accepted January 9, 2024)

Keywords: CdS, Elastic constants, Thermodynamic properties

1. Introduction

The applications of CdS is various, including thin films, single crystals, particles and nanoparticles. CdS is a direct bandgap material with excellent optical and photoelectric properties [1]. It is widely used as a window material for solar cells, it also has potential applications in new fields such as medical imaging technology, chemical analysis, photocatalysis and robotics [2]. Different forms (wurtzite structure WZ, rocksalt structure RS and zinc-blende structure ZB) of CdS were synthesized and their properties were studied experimentally [3, 4]. However, in theory, the research on this crystal material has not been published much and is not systematic [5]. In theory, there is no comprehensive analysis data for ZB-CdS crystal research, in particular, the theoretical results of the lack of mechanical and thermal properties have not yet been reported in detail, so the theoretical study on the mechanical and thermal properties of CdS crystal materials is carried out in this paper, the physical quantities involved include elastic constants, bulk modulus, shear modulus, Young's modulus, Poisson's ratio, heat capacity, thermal expansion coefficient, Debye temperature, etc.

* Corresponding author: guanhao1980@sina.com
https://doi.org/10.15251/CL.2024.211.39

2. Computational methods

In this paper, the first-principles method based on the plane wave pseudopotential is used to calculate the crystal structure and elastic properties of CdS with the aid of the CASTEP package [6]. In the calculation, the exchange correlation potential is calculated by the CA-PZ method of local density approximation (LDA)[7], and the Vanderbilt ultrasoft pseudopotential [8] is used with the cutoff energy of 450 eV for the considered structure. The *k* point meshes of 7×7×7 for cubic structure CdS is generated using the Monkhorst-Pack scheme.

3. Results and discussion

3.1. Structural properties

The lattice parameters of cubic phase CdS are obtained after structural optimization by many different calculation methods, and compared with the experimental and theoretical values. The optimized lattice parameters is shown in Table 1. The lattice parameters of the most stable structure of CdS is given: $a = b = c = 5.862$ Å. The optimized lattice parameter is close to the experimental value 5.8304 Å and the theoretical value 5.811 Å, and the relative error is 1.36%. The optimized lattice parameters are used in the subsequent calculation of the physical properties.

Table 1. The optimized lattice parameters of CdS by different methods.

	GGA-PEB	GGA-RPEB	LDA-CAPZ	GGA-PW91	GGA-WC	Exp. [9]	Theo.[10]
$a = b = c$(Å)	6.097	6.278	5.862	6.080	5.956	5.8304	5.811
Relative error	4.37%	7.13%	0.54%	4.11%	2.11%	—	—

3.2. Mechanical properties

The study of the elastic properties of materials allows us to explore many aspects of the material. The elastic constants is the quantity that characterizes the material's elasticity, which can be calculated by applying stress to the material and analyzing the resulting strain. In this paper, we calculate the CdS cell model under the simulated environment of 0 GPa, 2 GPa, 4 GPa, 6 GPa, 8 GPa, 10 GPa, and get the calculation data of relative elastic constants. The independent elastic constants of the cubic system are C_{11}, C_{44} and C_{12}. The elastic constant components must satisfy the Born mechanical stability condition. That is, the elastic constant satisfies the following relationship[11]:

$$\begin{aligned} &\widetilde{C}_{44} > 0 \\ &\widetilde{C}_{11} - \left|\widetilde{C}_{12}\right| > 0, \\ &\widetilde{C}_{11} + 2\widetilde{C}_{12} > 0, \end{aligned} \tag{1}$$

$$\widetilde{C}_{\alpha\alpha} = \widetilde{C}_{\alpha\alpha} - P, \widetilde{C}_{12} = C_{12} + P$$

Table 2. The calculated elastic constants C_{ij} (GPa), bulk modulus B (GPa), shear modulus G (GPa), Young's modulus E (GPa), Poisson's ratio υ, B/G of CdS at different pressures.

Pressure(GPa)	C_{11}	C_{44}	C_{12}	B	G	E	υ	B/G
0	83.43	34.97	62.16	69.20	21.73	59.01	0.358	3.185
	80.19[a]	27.49[a]	58.92[a]	66.01[a]				
	89.38[b]	39.11[b]	53.52[b]					
2	91.0	31.13	72.0	78.35	19.39	53.73	0.386	4.042
4	98.41	30.07	81.76	87.32	18.04	50.64	0.403	4.839
6	105.71	22.49	91.39	96.17	14.24	40.71	0.430	6.754
8	112.52	21.55	100.57	104.59	13.18	37.95	0.444	7.935
10	119.40	19.94	109.83	113.02	11.34	32.92	0.452	9.968

[a]Ref.[5], [b]Ref.[12]

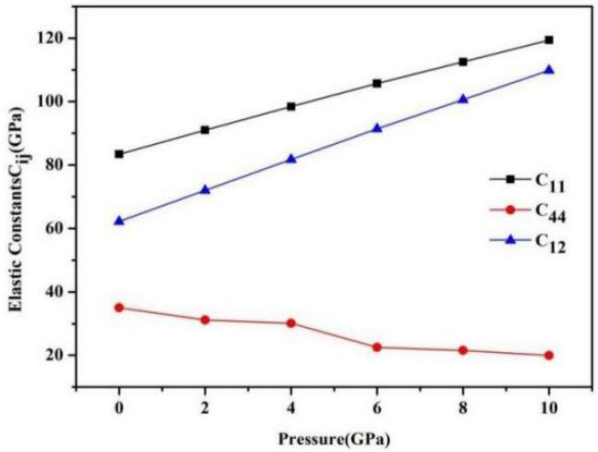

Fig. 1 The C_{ij} of CdS at different applied pressures.

As can be seen in Fig. 1, the independent elastic constants C_{11} and C_{12} of cubic CdS increase significantly with increasing pressure at 0-10 GPa. However, C_{44} gradually decreased with the increase of pressure from 0 to 10 GPa, but the decreasing trend was not obvious, which indicated that pressure had little effect on C_{44} compared with C_{11} and C_{12}, but their values always satisfy the condition of mechanical stability, which means that the crystal structure of CdS has mechanical stability. From Table 2, it can be seen that CdS is in the mechanical stable in the range of 0-10 GPa, the physical parameters such as shear modulus G, bulk modulus B, Young's modulus E and B/G were calculated by Voigt-Reuss-Hill method [13-15] . The above parameters are presented in Table 2. According to Voigt-Reuss-Hill approximation, the shear modulus G and bulk modulus B of cubic system are calculated as follows:

$$B_V = B_R = \frac{C_{11} + 2C_{12}}{3} \tag{2}$$

$$B_H = \frac{B_V + B_R}{2} \tag{3}$$

$$G_V = \frac{C_{11} - C_{12} + 3C_{44}}{5} \tag{4}$$

$$G_R = \frac{5(C_{11} - C_{12})C_{44}}{4C_{44} + 3(C_{11} - C_{12})} \tag{5}$$

$$G_H = \frac{G_V + G_R}{2} \tag{6}$$

Young's modulus E and Poisson's ratio υ:

$$E = \frac{9BG}{3B + G} \tag{7}$$

$$\upsilon = \frac{1}{2}\left(1 - \frac{E}{3B}\right) \tag{8}$$

According to the calculation results of B, G and E, the corresponding relation as shown in Fig. 2. We calculate the bulk modulus (B), shear modulus (G), Young's modulus (E) , Poisson's ratio (υ), and B/G of CdS in the pressure range of 0-10 GPa. As shown, B increases monotonously with increasing pressure and G and E decrease monotonously with increasing pressure. The calculated results show that the bulk modulus B is much larger than the shear modulus G at different pressures, so the compressive strength of CdS is stronger than its shear strength. In addition, the resistance to deformation of solid materials is characterized by Young's modulus E, from Fig. 2, Young's modulus E decreases with the increase of pressure, which shows that the crystal stiffness decreases with the increase of pressure. Unfortunately, there is no CdS experimental data and theoretical data to compare. As we all know, the brittleness or ductility of the materials has a great influence on its application in actual technical application. According to the Pugh standards of mechanical behavior of crystals, the determination of whether a solid material is ductility and brittleness is based on the ratio of B/G of bulk modulus B and shear modulus G, if the value of B/G is greater than 1.75, the material is ductility material, if the value of B/G is less than 1.75, the material is brittle material [16]. From the Table 2, it can be concluded that the B/G ratio of CdS is much larger than that of CdS crystal at 1.75 under different pressures. The results showed that the material exhibited ductility at 0-10GPa.

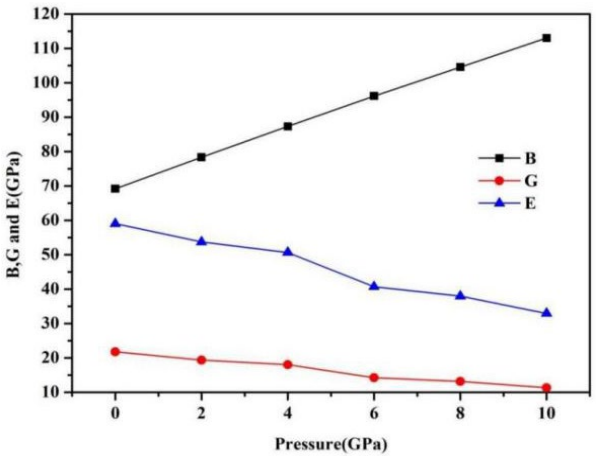

Fig. 2 The B, G and E of CdS at different applied pressures.

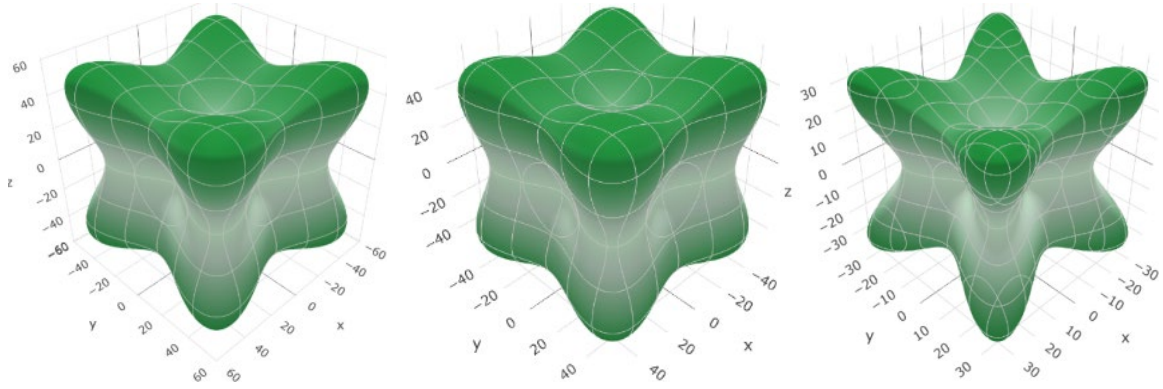

(a) *(b)* *(c)*

Fig. 3. The surface contours of Young's modulus of CdS ((a): 0 GPa, (b): 5 GPa, (c): 10 GPa). The unit is GPa.

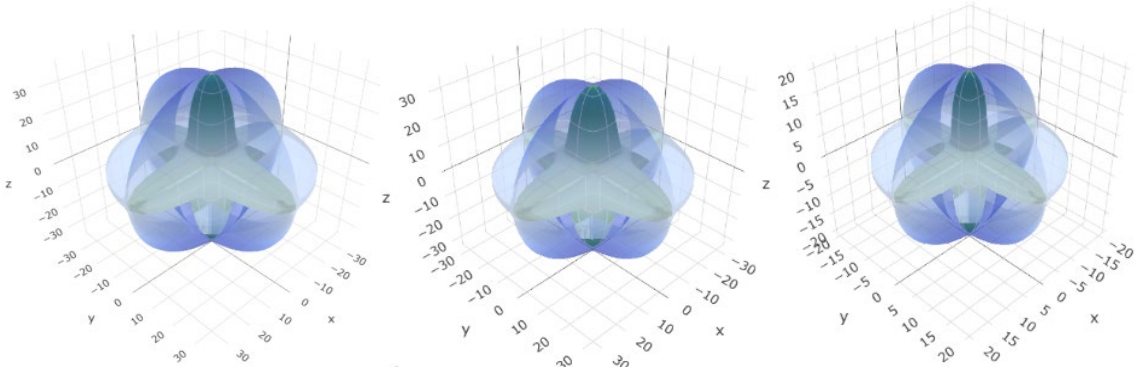

(a) *(b)* *(c)*

Fig. 4. The surface contours of Shear modulus of CdS ((a): 0 GPa, (b): 5 GPa, (c): 10 GPa). The unit is GPa.

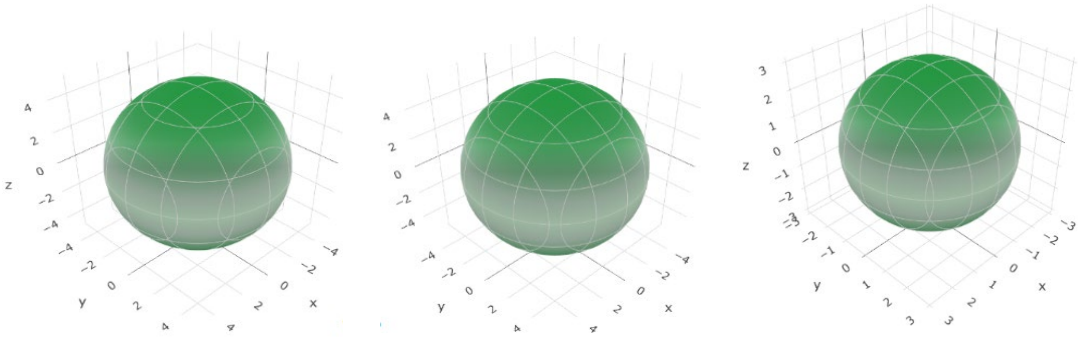

(a) *(b)* *(c)*

Fig. 5. The surface contours of linear compressibility of CdS ((a): 0 GPa, (b): 5 GPa, (c): 10 GPa). The unit is TPa^{-1}.

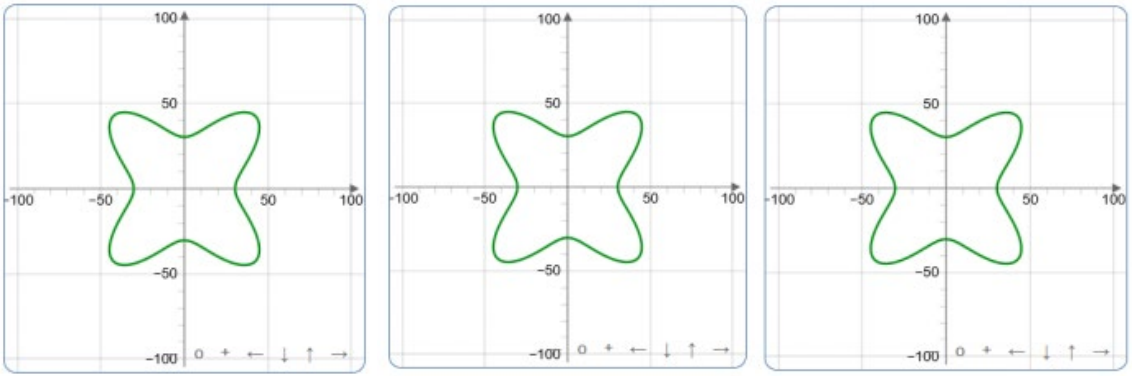

(a)

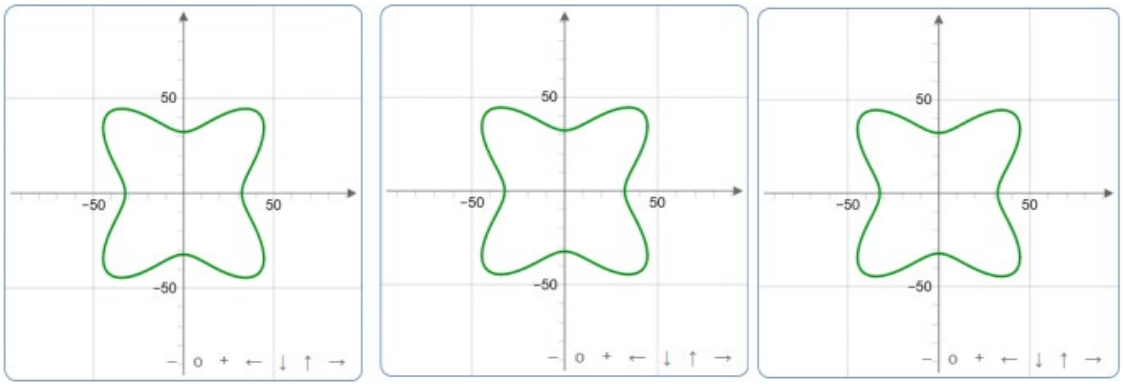

(b)

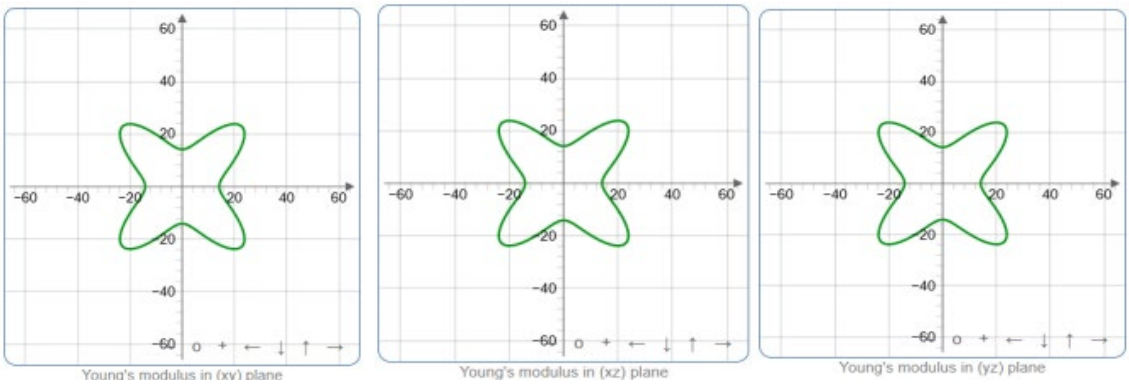

(c)

Fig. 6. Projections of Young's modulus in xy, xz, and yz planes of CdS. ((a): 0 GPa, (b): 5 GPa, (c): 10 GPa); The unit is GPa.

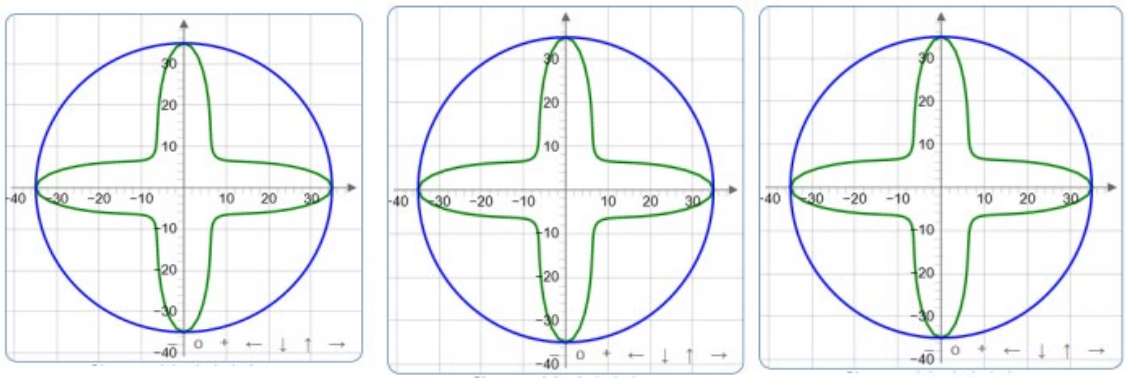

(a)

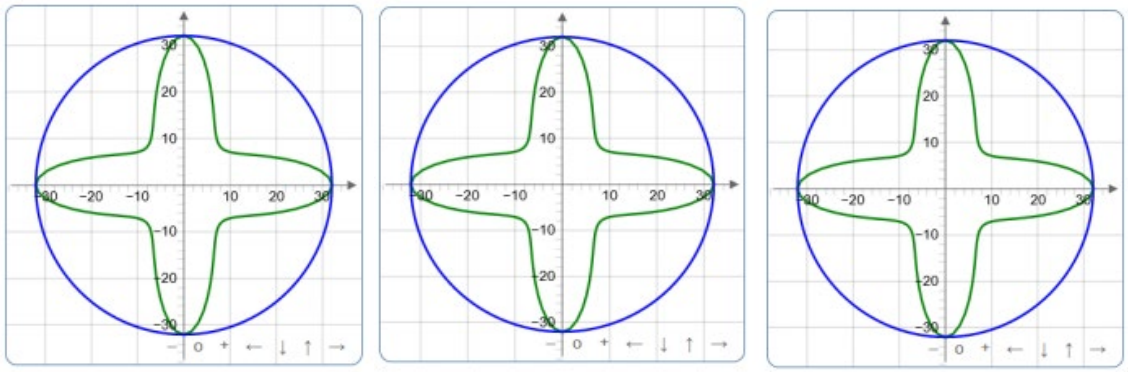

(b)

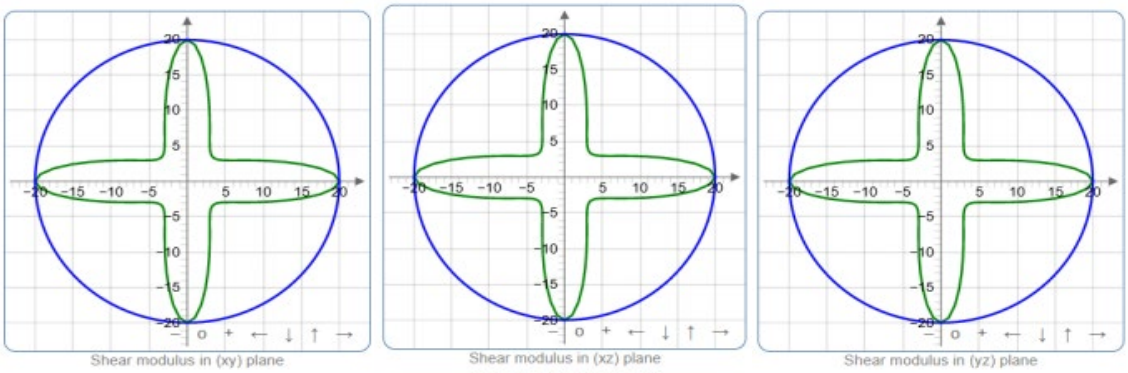

(c)

Fig. 7. Projections of Shear modulus in xy, xz, and yz planes of CdS. ((a): 0 GPa, (b): 5 GPa, (c): 10 GPa). The unit is GPa.

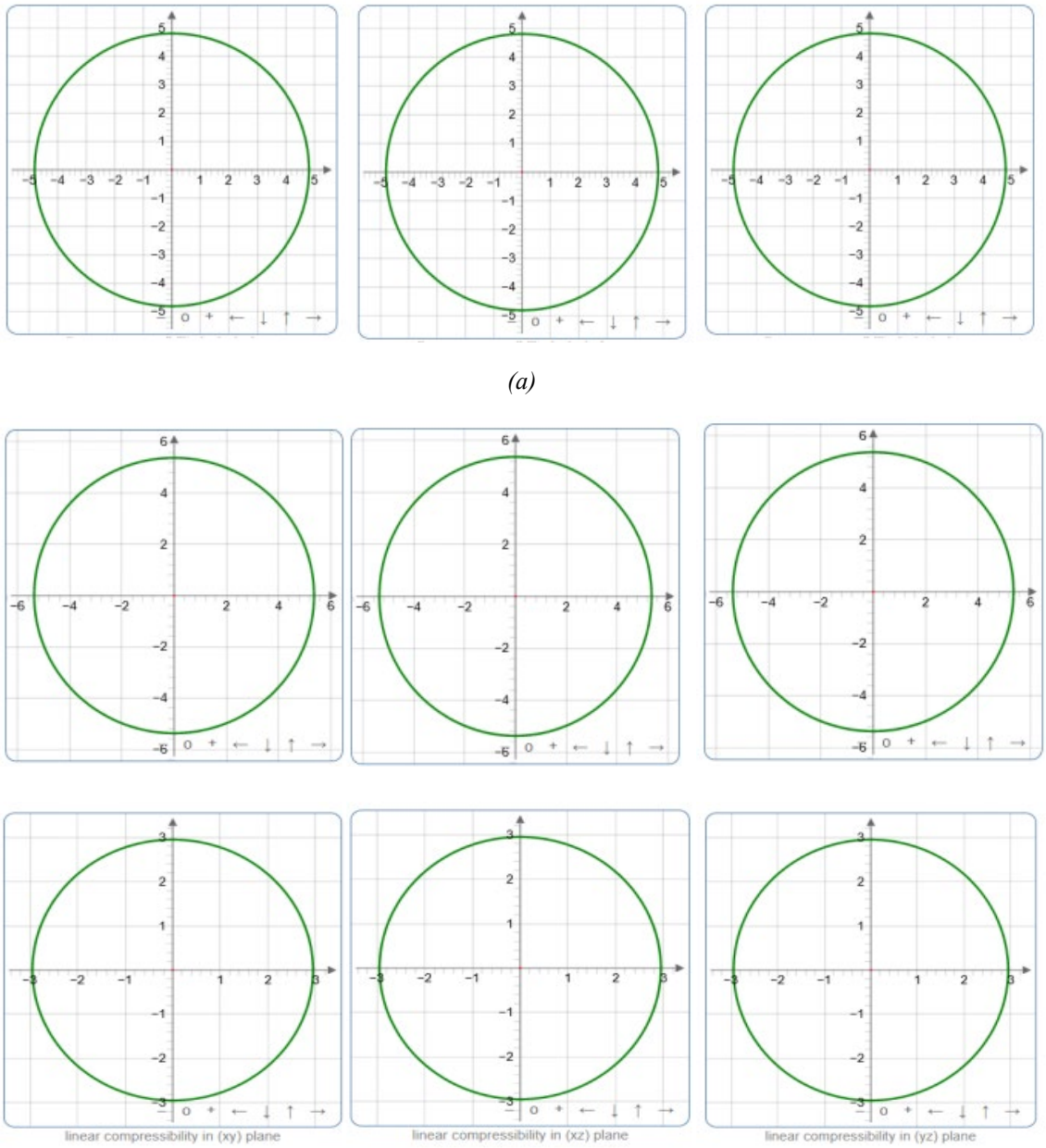

(a)

Fig. 8 Projections of linear compressibility in xy, xz, and yz planes of CdS. ((a): 0 GPa, (b): 5 GPa, (c): 10 GPa). The unit is TPa^{-1}.

In order to study the elastic anisotropy of CdS, the three-dimensional (3D) surface structures of linear compression coefficient β, shear modulus G, Young's modulus E are determined [17]. The anisotropy of the material shows a three-dimensional (3D) spherical structure. Figs.3-5 show the 3D spherical structures of Young's modulus E, shear modulus G, linear compressibility β at 0GPa, 5GPa, and 10GPa, respectively. It is clear that the 3D images of Young's modulus E, shear modulus G are very different from those of the spheres, indicating significant anisotropy. Figs 6-8 show the projections of Young's modulus E, shear modulus G, linear compressibility β on the xy, xz, and yz planes. The greater the deviation from the circle, the stronger the anisotropy. The projection of Young's modulus E and shear modulus G on different crystal planes deviates from the circle obviously, which further proves that CdS has strong anisotropy.

3.3. Thermodynamic properties

We calculated the total energy E and the corresponding volume V of the CdS according to the Birch-Murnaghan equation of state[18], as shown in Fig. 9. From Fig. 9, we can see that when the volume of CdS is 1335.5 $Bohr^3$, the total energy of cell is at the lowest level, which is the most stable state.

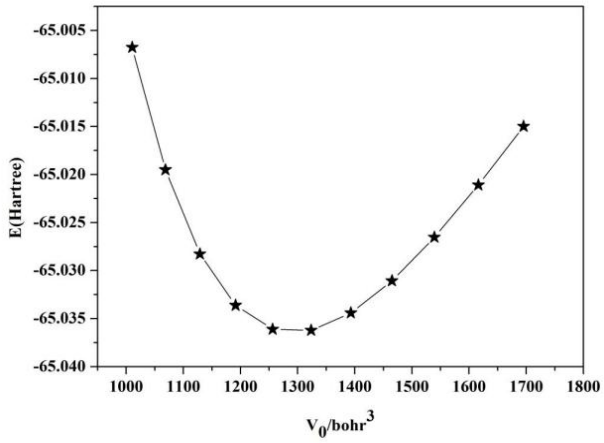

Fig. 9. Total energies E as the function of the unit cell volumes V_0 for CdS.

When studying the thermodynamic properties of materials, its thermodynamic properties at high temperature and high pressure are the focus of research, the temperature and pressure are the two most important factors that affect the thermodynamic properties in the real environment, so it is necessary to study the thermodynamic properties of materials in these two environments.

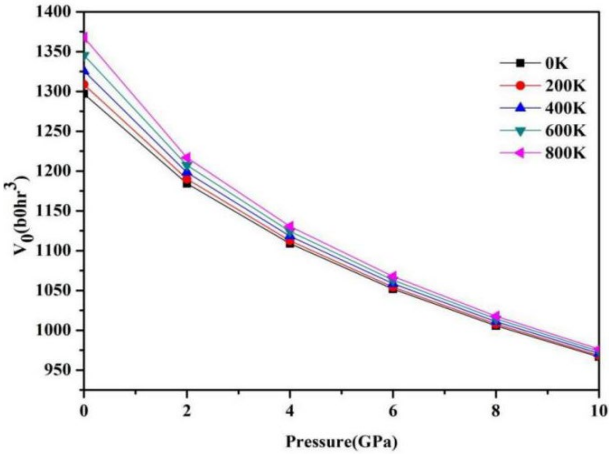

Fig. 10. Volume versus pressure at different temperatures.

Fig. 10 shows that volume V_0 continues to contract at various temperatures with increasing pressure, with a more pronounced contraction trend than that caused by temperature. It follows that pressure has a greater effect on volume V than temperature. Fig. 11 shows the effect of temperature on the heat capacity C_V at a fixed pressure, with an increase in temperature causing an increase in the heat capacity C_V at the same pressure. In this figure, the trend of increasing heat capacity C_V over the temperature range of 0-400 K is very clear, whereas after 400 K the heat

capacity curve continuously converges to a Dulong-Petit limit value, this phenomenon is caused by the anharmonic effect. However, from Fig.11 and 12, we can see that the C_V and C_P trends are quite similar when the temperature is below 200 K, however, when the temperature is higher than 200 K, C_P still has an increasing trend at 0 GPa and the increasing range is obvious.

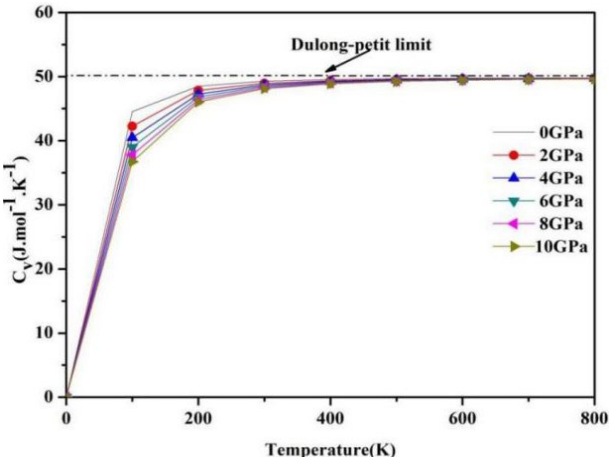

Fig. 11. The temperature dependence of C_V at different pressures.

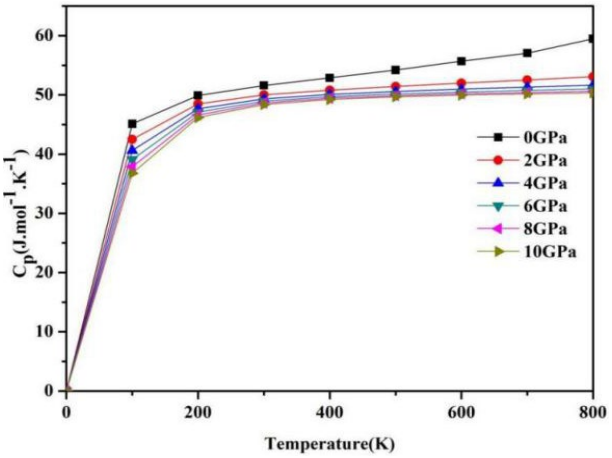

Fig. 12. The temperature dependence of C_P at different pressures.

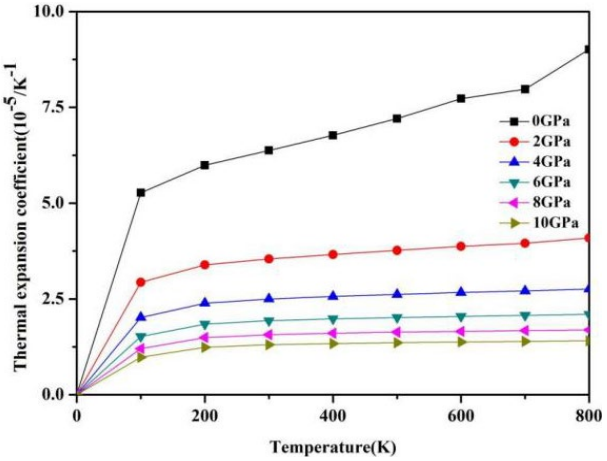

Fig. 13. The temperature dependence of thermal expansion coefficient at different pressures.

From Fig. 13, the pressure increases thermal expansion coefficient when the temperature is below 100K. After 100 K, the increase continues but the rate gradually flattens out. At 2-10 GPa, the thermal expansion coefficient also increased, but not significantly, and reached a stable value when the temperature was above 600K. But at 0 GPa, the thermal expansion coefficient still increases as the temperature continues to rise above 600K.

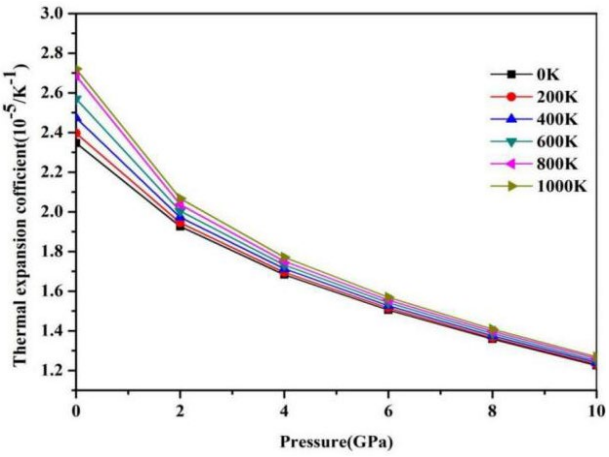

Fig. 14. The pressure dependence of thermal expansion coefficient at different temperatures.

From Fig. 14, it can be seen that the thermal expansion coefficient decreases rapidly at temperatures of 0K, 200K, 400K, 600K, 800K when the pressure changes from 0 GPa to 10 GPa, however, the larger the pressure, the more gentle the trend of reduction. At the same time, the values are also close to each other. This shows that under the conditions of high temperature and high pressure, the effect of temperature and pressure on the thermal expansion coefficient continues to weaken.

Table 3. The calculated entropy S, Debye temperature θ and Grüneisen constant γ of CdS at different temperatures and pressures.

T/K	*P*/GPa	0	2	4	6	8	10
0	*S*	0	0	0	0	0	0
	θ	153.42	186.11	209.6	228.01	243.12	255.85
	γ	2.347	1.926	1.683	1.505	1.358	1.225
200	*S*	81.48	71.62	65.80	61.75	58.702	56.31
	θ	150.24	184.38	208.38	227.11	242.44	255.33
	γ	2.397	1.945	1.695	1.514	1.364	1.231
400	*S*	117.10	106.10	99.82	95.45	92.17	89.58
	θ	145.58	181.86	206.56	225.74	241.38	254.48
	γ	2.474	1.973	1.713	1.527	1.375	1.24
600	*S*	139.11	126.91	120.32	115.78	112.37	109.70
	θ	140.22	179.2	204.67	224.3	240.27	253.61
	γ	2.57	2.004	1.732	1.541	1.386	1.249
800	*S*	155.60	142.00	135.08	130.38	126.87	124.13
	θ	134.24	176.38	202.74	222.84	239.13	252.7
	γ	2.687	2.037	1.751	1.555	1.397	1.259
1000	*S*	167.33	153.84	146.67	141.80	138.20	135.40
	θ	132.61	173.83	200.77	221.37	237.99	251.79
	γ	2.721	2.068	1.771	1.569	1.408	1.268

From Table 3, it can be observed that the value of entropy increases with the constant increase of pressure and temperature, while the value of Grüneisen constant increases, while the Debye temperature decreases gradually with the opposite trend. On the contrary, when the temperature is constant, the obtained temperature value increases, but the entropy and Grüneisen constant decrease.

4. Conclusions

The structural and elastic properties of CdS is systematically studied by first-principles method. The equilibrium structure parameters of CdS is obtained by optimizing the system. The calculated results are in good agreement with the experimental and theoretical values. Based on the calculated elastic constants of CdS, Voigt-Reuss-Hill approximation method is used to calculate a series of physical parameters which describe the mechanical properties of CdS, such as bulk modulus B, Young's modulus E, shear modulus G, Poisson's ratio υ, etc. The thermodynamic properties of CdS was studied by using Debye quasi-harmonic model. The Debye temperature, heat capacity C_V, thermal expansion coefficient, and Grüneisen parameters of CdS was calculated at pressures of 0-10 GPa and temperatures of 0-800 K, a change in temperature or pressure.

References

[1]Sahay P P, Nath R K, Tewari S 2007 Cryst. Res. Technol. 42 275; https://doi.org/10.1002/crat.200610812

[2]Greenwood N N, Earnshaw A 1997 Chemistry of the Elements (2nd Ed.) (Oxford:Butterworth-Heinemann)

[3]Weber M J 1986 Handbook of Laser Science and Technology (Vol. III) (Cleveland: CRC Press)

[4]Benkhettou N, Rached D, Soudini B, Driz M 2004 Phys. Status Solidi B 241 101

[5]P. Zhou, X.Q. Wang, M. Zhou, C.H. Xia, L.N. Shi, C.H. Hu, Acta Physica Sinica, 62, 087104(2013)https://doi.org/10.7498/aps.62.087104

[6]S. J. Clark, M. D. Segall, C. J. Pickard, Z. Kristallogr 220,567 (2005); https://doi.org/10.1524/zkri.220.5.567.65075

[7] J. P. Perdew, A. Zunger, Phys. Rev. B 23; 5048(1981)https://doi.org/10.1103/PhysRevB.23.5048

[8]D. Vanderbilt Phys. Rev. B 41, 7892(1990); https://doi.org/10.1103/PhysRevB.41.7892

[9]D. Rodic, V. Spasojevic, A. Bajorek, P. Onnerud, Journal of Magnetism and Magnetic Materials 152,159 (1996); https://doi.org/10.1016/0304-8853(95)00435-1

[10]Yeh C Y, Lu Z W, Froyen S, Zunger A Phys. Rev. B 46, 10086(1992); https://doi.org/10.1103/PhysRevB.46.10086

[11]M. Born, K. Huang, Dynamical Theory of Crystal Lattices(Oxford: Clarendon) 1954.

[12]K. Wright, J. D. Gale, Interatomic potentials for the simulation of the zinc-blende and wurtzite forms of ZnS and CdS: Bulk structure, properties, and phase stability, Phys. Rev. B 70, 035211(2004); https://doi.org/10.1103/PhysRevB.70.035211

[13] W. Voigt Lehrbuchder Kristallphysik Teubner Leipzig (1928)

[14] A. Reuss , Z. Angew. Math. Mech. 9, 49 (1929); https://doi.org/10.1002/zamm.19290090104

[15] R. Hill, Proc. Phys. Soc. 65, 349 (1952); https://doi.org/10.1088/0370-1298/65/5/307

[16] S. F. Pugh, Philos. Mag. 45, 823 (1954); https://doi.org/10.1080/14786440808520496

[17]R. Gaillac, P. Pullumbi, F.-X. Coudert,J. Phys. Condens. Matter 28, 275201(2016); https://doI.org/10.1088/0953-8984/28/27/275201

[18]M. A. Blanco, A. Martín Pendás, E. Francisco, J. M. Recio, R.Franco, J. Mol. Struc-Theochem. 368, 245(1996); https://doi.org/10.1016/S0166-1280(96)90571-0